In vivo Imaging of Kurtosis Tensor Eigenvalues in the Brain at 3 T

E. E. Sigmund[1], M. Lazar[1], J. H. Jensen[1], and J. A. Helpern[1]
[1]Radiology, New York University, New York, NY, United States

Background

Diffusion tensor imaging (DTI), a gaussian anisotropic diffusion model, provides mean diffusivity (MD) and fractional anisotropy (FA) metrics that describe diffusion in brain tissue (white and gray matter). However, the widely recognized non-gaussian diffusion behavior in tissue has motivated higher order schemes (q-ball, HARDI, DSI) to accurately describe the tissue structure. In generalized DTI, higher order tensors are invoked to represent the orientational diffusion profile [1-3]. Diffusional kurtosis imaging (DKI) measures the displacement non-gaussianity or "kurtosis" [4,5]. The directionally averaged mean kurtosis (MK) has been shown to be a potentially valuable disease marker in such illnesses as Alzheimer's and ADHD [6,7]. Recent work has also used kurtosis projections along the diffusion tensor [8], and the kurtosis tensor has been used to estimate the full orientation distribution function (ODF) [9]. Another strategy, analogous to the principal diffusivities of the diffusion tensor, is to seek eigenvalues/tensors/vectors of the kurtosis tensor as its characteristic features. Though this is challenging for a rank-4 object, there are mathematical prescriptions for deriving such parameters [10,11]. The present study employed spectral decomposition [10] of the diffusion kurtosis tensor, in order to understand the kurtosis variation in the brain and supplement tractography techniques.

Methods

Scans were performed on a healthy volunteer in a full body Siemens Tim Trio 3 T scanner with a 12-channel head coil. DKI data used a twice-refocused bipolar diffusion gradient EPI sequence (2 x 2 x 2.5 mm resolution, 100 x 100 matrix, 50 slices, iPat = 2, 64 directions, b = 0 (11 avgs.) ,1000, 2000 s/mm^2 (2 avgs ea.)) Analysis was performed using code written in Igor Pro. For each direction $\hat{n}$, apparent diffusion ($D(\hat{n})$) and apparent kurtosis ($K(\hat{n})$) were extracted:

$$\ln S = \ln S_0 - bD(\hat{n}) + \frac{1}{6}b^2 D(\hat{n})^2 K(\hat{n}) \qquad (1.1)$$

Apparent diffusion coefficients were used to estimate the diffusion tensor D_{ij}, and the kurtosis tensor W_{ijkl} was determined according to:

$$K(\hat{n}) = \frac{\bar{D}^2}{D(\hat{n})^2} \sum_{i,j,k,l=1}^{3} \hat{n}_i \hat{n}_j \hat{n}_k \hat{n}_l W_{ijkl} \qquad (1.2)$$

Note that this definition implies qualitative distinctions between apparent kurtosis and kurtosis tensor. The spectral decomposition described in ref. [10] was used to estimate 6 eigenvalues σ_k^2 and eigentensors E^k (3 x 3) of the kurtosis tensor W. Eigentensors' eigenvalues γ_i^k and eigenvectors v_i^k (3 x 1) were also calculated. These were used to construct composite "eigensurfaces" representing the projection P of W along $\hat{r}$ by

$$P(\hat{r}) = \sum_{k=1}^{6} \left(\sum_{i=1}^{3} \sigma_k \gamma_i^k \left(\hat{r} \cdot v_i^k \right)^2 \right)^2 \qquad (1.3)$$

Maps were generated of the standard DTI indices, the kurtosis eigenvalues σ_k^2 and their arithmetic mean, the experimental mean kurtosis MK, and eigensurface maps of several areas of the brain.

Results

Figure 1 shows parameter maps for a single slice. DTI maps MD, FA, and directionally encoded colormaps show standard contrast in white and gray matter. MK shows higher values in white and gray matter, though both are nonzero. Very similar contrast is shown in the image of the mean of the kurtosis eigenvalues. The eigenvalue maps show striking gray matter / white matter contrast as well, particularly for the principal eigenvalue. White matter kurtosis spans a large range of values across the eigenvalue set ($0.1 < \sigma^2 < 2$), while gray matter values occupy a smaller range ($0.3 < \sigma^2 < 1.2$). Figure 2 shows kurtosis eigensurfaces for a highlighted region of at the level of the pons; these surfaces qualitatively indicate crossing longitudinal and transverse fibers. An eigensurface at a frontal white matter fiber crossing is shown along with the eigenvectors v_i^k derived from the highest and lowest kurtosis eigenvalues. These vectors point out the dominant lobes of the eigensurface.

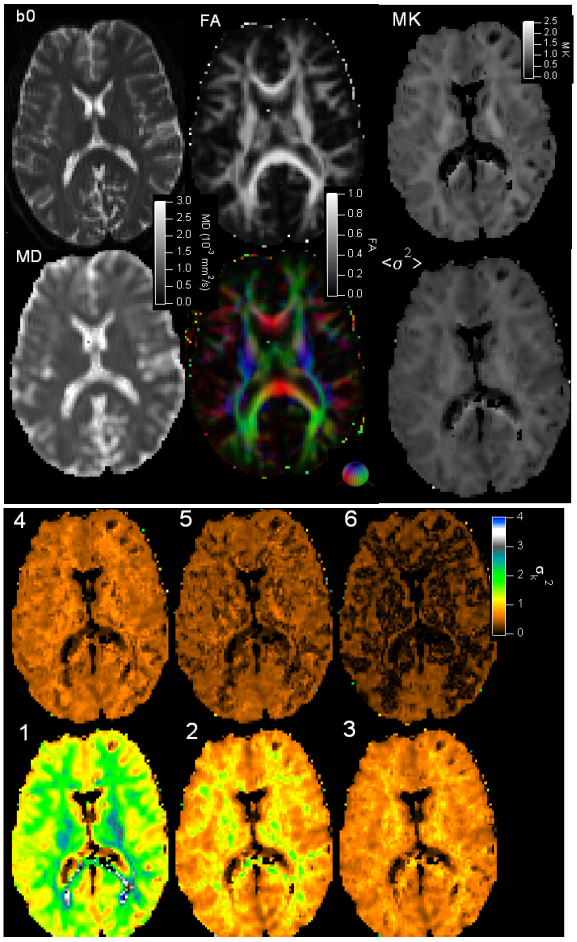

Figure 1: Diffusion parameter maps. Top : DTI indices MD, FA, and direction encoded colormap. MK : experimental mean kurtosis. $\langle\sigma^2\rangle$: mean of kurtosis eigenvalues. Bottom: Kurtosis eigenvalue maps (1-6).

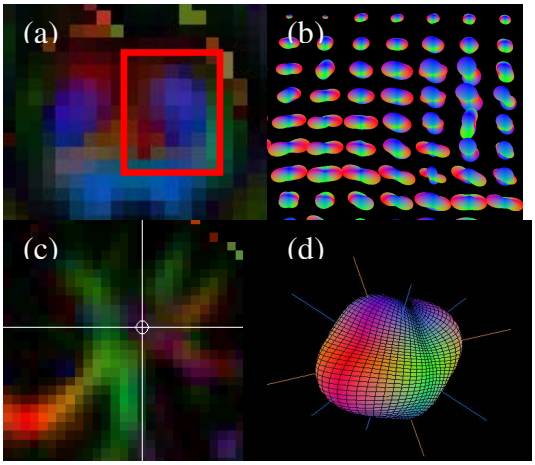

Figure 2. (a) Region of pons for eigensurface display in (b). (c) Frontal white matter voxel for eigensurface in (d), which includes eigenvectors v_i^k for the highest (blue) and lowest (brown) kurtosis eigenvalues.

Discussion

Spectral decomposition allows a deeper inspection of features of the kurtosis tensor both in magnitude and orientation. White matter's structural anisotropy, including areas of fiber crossing, gives it a higher dynamic range of kurtosis eigenvalues than in gray matter. The composite eigensurfaces seem to be sensitive to multiple intersecting fiber species, as shown in Figure 2, where multiple eigenvectors identify characteristic displacement features. This behavior may also arise from anisotropic barrier density (which impacts kurtosis). One application of this processing would involve using these vectors (e.g., from the principal kurtosis eigenvalue) for tractography, which future work will investigate.

References

[1] Liu CL et.al. MRM 2004;51(5):924-937. [2] Jayachandra MR et.al. MRM 2008;60(5):1207-1217. [3] Ozarslan E et.al. MRM 2003;50(5):955-965. [4] Jensen JH & Helpern JA ISMRM 2003;11:2154. [5] Jensen JH et.al. MRM 2005;53(6):1432-1440. [6] Lu H et al. ISMRM 2006;14:723. [7] Helpern JA et al. ISMRM 2007;15:1580. [8] Wu EX et.al. Neuroimage 2008;42 (1):122-134. [9] Lazar M et.al. MRM 2008;60(4):774-781. [10] Basser PJ et.al. Signal Processing 2007;87(2):220-236. [11] Qi LQ et.al. J. Comp. Appl. Math. 2008;221(1):150-157.